ELSEVIER

Journal of Chromatography A, 872 (2000) 227–246

JOURNAL OF CHROMATOGRAPHY A

www.elsevier.com/locate/chroma

Investigation of Cr(III) hydrolytic polymerisation products by capillary electrophoresis–inductively coupled plasma-mass spectrometry

Ian I. Stewart[a], John W. Olesik[b,*]

[a]*National Research Council Canada, Montreal Road Campus, M-12, Ottawa, Ontario K1A 0R6, Canada*
[b]*Laboratory for Plasma Spectrochemistry, Laser Spectroscopy and Mass Spectrometry, Department of Geological Sciences, Ohio State University, Columbus, OH 43210, USA*

Received 20 September 1999; accepted 4 November 1999

Abstract

The development of a new method for the determination of Cr(III) hydrolytic polymerisation products using capillary electrophoresis–inductively coupled plasma mass spectrometry (CE–ICP-MS) is described. The results indicate that CE–ICP-MS can be used to separate and detect monomeric and polymeric Cr(III) species. The various species migrate through the capillary at a rate proportional to their equilibrium distribution, which is dictated by the solution pH, metal ion concentration and ageing period. In general, the data suggest that the relative mobility follows the order trimer>dimer> monomer. The experimentally determined speciation shows a good qualitative agreement with that described in the literature. Independent confirmation of the presence of polymeric Cr(III) species was performed by ionspray mass spectrometry.

Keywords: Instrumentation; Capillary electrophoresis–mass spectrometry; Chromium; Metal cations; Polymers

1. Introduction

The hydrolysis of chromium(III) is a fundamental process that occurs in most aqueous solutions and is often a natural precursor to the formation of more complex polynuclear (polymeric) species or oligomers [1]. The importance of these species is becoming increasingly recognised in a variety of systems and matrices. For example, the formation of polymeric species in natural waters [2] can have a significant impact on the mobilisation, transport and fate of Cr(III) in the environment. This is especially true in waste sites and industrial effluents, which are major sources of chromium in the environment [3–5]. As well, the formation, type and purity of polymeric species in electroplating solutions [6], tanning [7,8] and polymerisation processes [9,10] can be of critical importance. Although, little direct information is known on the impact of polymeric species in biological systems, their formation and presence is known to compete with Cr(III)–ligand complexation which can interfere with the biological function of chromium [11]. As such there is now a growing need for the development of methods capable of the accurate determination of these polymeric species.

*Corresponding author. Tel.: +1-614-292-6954; fax: +1-614-292-7688.
E-mail address: olesik.2@osu.edu (J.W. Olesik)

0021-9673/00/$ – see front matter
PII: S0021-9673(99)01164-4

The chemistry of polymeric Cr(III) species has been discussed extensively in the literature. This includes the characterisation of smaller oligomers such as dimers, trimers, tetramers and hexamers [12–29] as well as other larger oligomeric species [30]. Although the speciation and formation mechanisms of each oligomer can vary significantly, oligomeric species are generally classified as $Cr_q(OH)_p^{(3p-q)+}$ where q refers to the general nuclearity of the oligomer and p refers to the number of hydroxyl ligands (cf. Ref. [14]). The hydrolytic polymerisation of chromium is typically dependent on the metal ion concentration, solution pH, solution matrix and the solution history or ''ageing'' period.

Of the oligomers, the monomer ($q=1$), represents the simplest form and is a fundamental building block of more complex polymeric species such as the dimer ($q=2$) or trimer ($q=3$). The process is pH dependent, and is initiated by the formation of monomeric the Cr(III) hydroxyl species. A brief summary of the formation of various hydrolytic monomer species is given below in reactions (1)–(4). Formation constants can be found in Refs. [1,14,28,29].

$$Cr(H_2O)_6^{3+} \rightarrow Cr(OH)(H_2O)_5^{2+} + H^+ \quad (1)$$

$$Cr(OH)(H_2O)_5^{2+} \rightarrow Cr(OH)_2(H_2O)_4^{+} + H^+ \quad (2)$$

$$Cr(OH)_2(H_2O)_4^{+} \rightarrow Cr(OH)_3(H_2O)_3 + H^+ \quad (3)$$

$$Cr(OH)_3(H_2O)_3 \rightarrow Cr(OH)_4(H_2O)_2^{-} + H^+ \quad (4)$$

For kinetically inert centres such as Cr(III), protonation/deprotonation reactions are fast while substitution reactions (or exchange) involved in the formation of oligomers are slow [16]. The addition of base therefore rapidly deprotonates the Cr^{3+} aquo-ion providing a conjugate base that is more reactive in the substitution processes necessary for the formation of oligomers. Acidification will reprotonate species and retard further polymerisation.

Reactions (5)–(9) provide a summary of a number of polymeric species reported in the literature, with examples of possible formation mechanisms.

$$2Cr(OH)(H_2O)_5^{2+} \xrightarrow{\text{DIMERISATION}} Cr_2(OH)_2(H_2O)_8^{4+} + 2H_2O \quad (5)$$

$$\text{Monomer} + \text{Dimer} \rightarrow \text{Trimer}\quad \text{e.g. } Cr_3(OH)_6(H_2O)_9^{5+} \quad (6)$$

$$\text{Monomer} + \text{Trimer} \rightarrow \text{Tetramer}\quad \text{e.g. } Cr_4(OH)_8(H_2O)_{10}^{6+} \quad (7)$$

$$\text{Dimer} + \text{Trimer} \rightarrow \text{Pentamer}\quad \text{e.g. } Cr_5(OH)_8(H_2O)_{12}^{7+} \quad (8)$$

$$\text{Trimer} + \text{Trimer} \rightarrow \text{Hexamer}\quad \text{e.g. } Cr_6(OH)_{10}(H_2O)_{14}^{8+} \quad (9)$$

The oligomers shown in reactions (5)–(9) represent fully protonated forms and typically only exist at low pH. Similar to the monomer, each of the oligomers will have equilibrium species distribution curves that are highly dependent on pH. In addition, the relative acidities of the various oligomers can vary significantly, for example, the dimer has a pK_{a_1} of 3.68, whereas the monomer ($Cr(H_2O)_6^{3+}$) has a pK_{a_1} of 4.29 [14]. A list of pK_a values for a number of oligomers has been provided by Stunzi and Marty [14].

Often, however, the absence of information on a samples' history and thermodynamic data make accurate speciation modelling a difficult and perhaps impractical task. As well, due to the quasi-stable nature of most polymeric species, it is difficult to assume in all cases that their reactivity is dictated by their equilibrium monomer species. An assessment of chemical speciation is therefore critical before any true understanding of an element's reactivity, transport or interaction within a particular environment can be achieved.

In the laboratory, solution based polymeric Cr(III) speciation can be monitored as a function of pH and time by potentiometric methods [12–27]. Further characterisation of test solutions is typically performed using open column cation-exchange chromatography (e.g., Sephadex) incorporating off-line UV–Vis detection [12–27]. For UV–Vis detection, the fractions are classified based upon the absorbance ratios (ca. 420 nm/ca. 580 nm) where the greater the ratio, the higher the order of the polymeric species [14]. A summary of the chromatographic methods used for the determination of polymeric Cr(III) speciation has been provided by Collins et al. [31]. In more recent studies, Saleh et al. [2], have employed flame atomic absorption spectrometry for off-

line quantitation of Cr containing fractions separated from pure and natural water samples using open column ion-exchange chromatography. The fractions were then further separated by non-suppressed ion chromatography and detected using UV–Vis methods. Similarly, Collins et al. [31] have used radiometric $^{51}Cr^{+}$ detection for off-line element selective detection in tandem with on-line HPLC–UV–Vis studies of Cr(III) polymeric speciation.

Although the on-line chromatographic methods described above are effective for research purposes, they do suffer from limitations. In particular, poor sensitivity and non-element specific detection associated with UV–Vis techniques can significantly limit the analytical performance. Additional off-line element specific detection is possible, however, it can further increase already long total analysis times. For example, Collins et al. [31], report analysis times for on-line separation and detection in excess of 50 min. In addition, specific interactions within the separation column can potentially modify semi-labile speciation and degrade the analytical accuracy of the measurement.

Theoretically, capillary electrophoresis–inductively coupled plasma mass spectrometry (CE–ICP-MS) should provide an effective means to separate and detect Cr(III) polymeric species in solution. Although the oligomers are considered thermodynamically unstable, research using ion-exchange chromatography [14] indicates that they can be separated and stored for short periods of time and therefore should be stable over the course of a CE–ICP-MS separation (~5 min). In addition, the quasi-stable oligomers formed [reactions (5)–(9)] will have structures (size, mass) that are characteristic of the degree of polymerisation (e.g., [17]). The charge states of these structures will be pH dependent and, similar to the monomer species, will exist as an equilibrium mixture.

Research using CE–ICP-MS for elemental speciation, has already revealed its ability to separate and detect species based upon different elements (inter-element) [32–37] and different species based upon the same element (intra-element) [32–36,38–45]. A significant portion of the CE–ICP-MS literature has also been devoted to interface design and development [33–37,46,47] and speciation errors [48]. The current status of CE–ICP-MS as a tool for elemental speciation has been summarised by Barnes [49] and Olesik [50] and in reviews by Sutton et al. [51] and Zoorob et al. [52].

Initial reports by Olesik et al. [32,33] have demonstrated the capability of CE–ICP-MS to separate and detect Cr(III) and Cr(VI) fractions in a given sample. Similarly, Mei et al. [53] have used CE coupled with inductively coupled plasma atomic emission spectrometry (ICP-AES) for the separation of Cr(III) and Cr(VI) fractions. In both cases, the element selective detection provided by either CE–ICP-AES or ICP-MS offers rapid analysis times ($<$10 min), with detection limits estimated to be between 1 and 10 ppb for both species. In contrast with other CE methods [54], CE–ICP-MS does not require the use of complexing agents or specific interactions to separate Cr(III) from Cr(VI) fractions in a single run, or other intra-element species for that matter. This is beneficial for maintaining accurate speciation information. A number of simple, non-complexing electrolyte salt solutions such as alkali, alkaline earth and lanthanide halides and nitrates have been used successfully by Olesik et al. [32,33] as separation electrolytes. Although, CE–ICP-MS has been used for the rapid, sensitive determination chromium fractions, there have been no reports in the literature on the separation and detection of Cr(III) polymeric species.

The purpose of this study is to evaluate the capability of CE–ICP-MS as a tool for hydrolytic Cr(III) speciation. In particular, using a solution with well-defined chemistry, is it possible to separate a Cr(III) fraction into its various oligomeric components (e.g., monomeric, dimeric, trimeric, etc.) and more importantly, determine if these species distributions are consistent with those theoretically expected. In answering these questions, the choice of separation electrolyte, including type, pH and concentration (conductivity), will be discussed in terms of optimum performance for the separation of polymeric species. As well, the importance of other experimental parameters such as voltage, sheath flow electrolyte, sheath electrolyte flow-rate and induced laminar flow-rate will be discussed in relation to speciation, resolution, sensitivity and satisfactory analysis time. Because elemental detection can provide only limited direct speciation information, reference to the literature, the use of internal markers and

independent methods such as ionspray mass spectrometry (ISMS) are used to help identify the separated species. Due to the preliminary nature of this research, the results presented are purely qualitative.

2. Experimental

2.1. Chemical reagents and preparation

Stock and sample solutions were prepared by dissolving analytical-grade solid reagents in ultra pure water (18 MΩ cm^{-1}) obtained from a Milli-Q water purification system (Millipore, Milford, MA, USA). Analytes include LiCl (Fisher), $CrCl_3 \cdot 6H_2O$ (Baker), $Co(NO_3)_2 \cdot 6H_2O$ (Baker), $Y(NO_3)_3 \cdot 6H_2O$ (Fisher), CsCl (Fisher) and $Ce(NO_3)_3 \cdot 6H_2O$ (Aldrich). The separation electrolyte used was $LaCl_3 \cdot 6H_2O$ (Aldrich). Where necessary, the solution pH was adjusted through the addition of small volumes of dilute HCl or dilute NaOH solution. A Beckman Ω 31 pH meter calibrated using pH 4, 7 and 10 standard solutions was used for all pH measurements. Conductivity measurements were performed using a Fisher Scientific Accumet Portable AP63 pH/mV/Ion Meter.

2.2. Capillary electrophoresis–inductively coupled plasma mass spectrometry

A schematic of the CE–ICP-MS sheath flow interface used for all measurements is shown in Fig. 1. The interface has been described previously by Kinzer et al. [33] and so only a brief description will be provided here. A fused-silica capillary (Polymicro Technologies; 60 cm×50 μm I.D.×356 μm O.D.) was fitted through the co-linear ends of a stainless steel tee (Upchurch Scientific Model U428) with a sleeve [Model F230 polyether ether ketone (PEEK)] to hold the fused-silica capillary on the inlet side. At the outlet, the capillary immediately passes through a section of stainless steel tubing (Upchurch Scientific U138, 5 cm×0.04 in. I.D.×0.06 in. O.D.; 1 in.= 2.54 cm). The tip of the capillary was inserted part-way into a Meinhard® high efficiency nebuliser

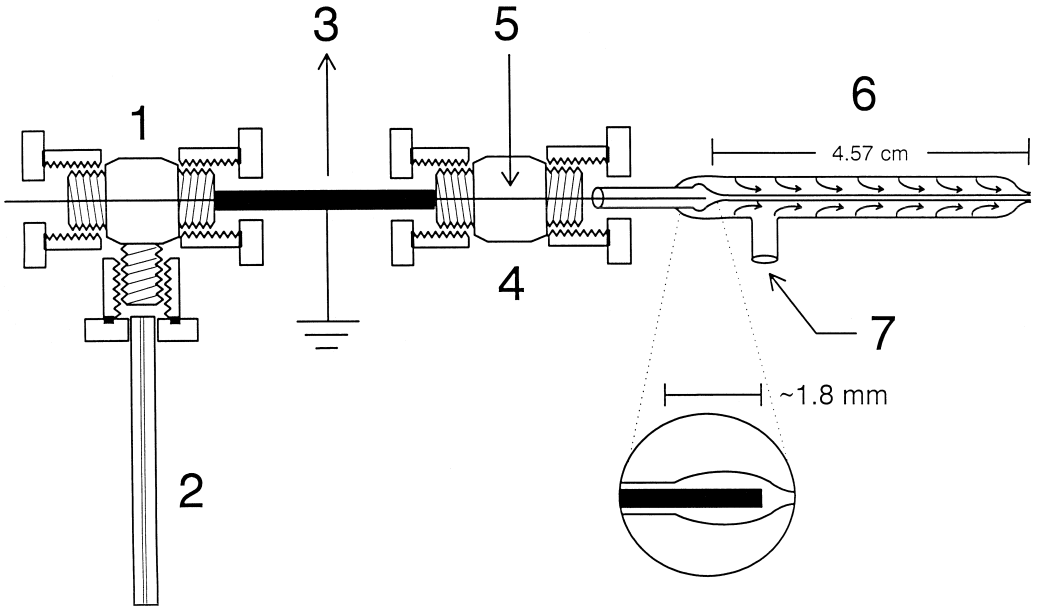

Fig. 1. Schematic diagram of the sheath-flow interface between the electrophoresis capillary and the concentric pneumatic nebuliser for CE–ICP-MS. (1) Stainless steel tee, (2) sheath flow electrolyte PEEK tubing from syringe pump, (3) stainless steel tubing with ground, (4) PTFE union, (5) fused-silica capillary, (6) Meinhard, HEN-170-AA nebuliser and (7) argon gas inlet. The inset shows the relative position of the capillary end inside of the nebuliser.

(HEN 170-AA) and fastened in place using a PTFE union (Upchurch Scientific U402). A syringe pump (KD Scientific) connected to the lower end of the stainless steel tee is used to deliver the sheath electrolyte from a glass syringe (Hamilton, 14.57 mm I.D.).

Electrical connection of the separation electrolyte and the high-voltage supply (Spellman, Model CZE 1000R d.c. power supply) was made through a platinum electrode. The high-voltage power supply ground was made at the stainless steel tubing that carries the sheath electrolyte solution. Because the sheath electrolyte solution flowing through the stainless steel sheath is in intimate contact with the effluent from the separation capillary a stable ground is maintained. Hydrodynamic injections were used for all measurements. Typically the sample was raised 11 in. above the outlet of the capillary for 60 s corresponding to an injection volume of 47 nl, or ~4% of the total capillary volume. For all measurements, 30 kV was used and depending on the separation electrolyte would usually correspond to currents less than 15 μA.

The nebuliser is fitted into an open conical spray chamber that is mounted onto the centre tube of a standard PE/Sciex Elan 6000 ICP-MS torch with a ball socket joint. An ELAN 6000 ICP-MS system was used for all measurements. Plasma (outer) and auxiliary (intermediate) gas flow-rates were 15 l/min and 1.4 l/min, respectively. Although optimised daily, the plasma power was typically 1200 W and the nebuliser gas flow-rate was ~0.80 l/min controlled by an external mass flow controller (Porter, Model 201-USVC). Parameters such as integration time, number of elements monitored and the number of replicates were chosen such that the total experiment time was longer than the time required for a given separation. Three to seven m/z values (elements) were measured using peak hopping with dwell times typically between 100 and 200 ms per peak.

2.3. Electrospray mass spectrometry

A PE/Sciex API 300 LC–MS–MS system incorporating an in-house source was used for all ionspray measurements. The source design however was based upon that described by previously by Olesik et al. [55]. The original stainless steel arm used to support the ion spray source in the API 300 was replaced with a new insulating arm manufactured from PTFE. A Meinhard® SB-30-A3 pneumatic nebuliser was mounted at the end of this arm. A fused-silica capillary (Polymicro Technologies; 60 cm×75 μm I.D.×150 μm O.D.) was inserted through the nebuliser, protruding 400 μm past the end of the tip. The fused-silica capillary was fastened in place at the inlet end of the nebuliser using a stainless steel reducing union. The union also provided an air-tight seal, preventing the entrainment of air through the central channel of the nebuliser. Solution was pumped through the capillary at 2 μl/min from a Hamilton gas-tight glass syringe (250 μl, Model 1725) using a syringe pump (Harvard Apparatus, Model 22). The API 300 software regulated the nitrogen gas supplied to the nebuliser, which was typically set at a value of 9. High-voltage from the API 300 was applied to the stainless steel–liquid junction at the capillary–syringe union. Under normally operating conditions the voltage was between +4 and 5 kV and the capillary tip was positioned approximately 20 mm from the front plate and 5 mm off axis (to the right looking at the front plate). Typical values for the curtain gas flow-rate, sampling orifice voltage, and ring electrode voltage were 6.50 and 200 V, respectively. For MS–MS experiments a collision activated dissociation (CAD) gas pressure corresponding to a software setting of 2 was used. This source design is particularly effective in generating consistent stable charged aerosol sprays from purely aqueous in either positive or negative ion mode.

3. Procedure

With reference to Fig. 1, argon gas exiting the nebuliser will induce a natural aspiration through its central solution uptake capillary. As a consequence, liquid will flow from the separation electrolyte reservoir through the electrophoresis capillary to the nebuliser tip (induced laminar flow) at a rate proportional to the natural aspiration rate. When the sheath electrolyte is pumped around the capillary tip towards the nebuliser tip it reduces the effect of natural aspiration through the electrophoresis capillary and,

therefore, the accompanying degradation in separation efficiency due to induced laminar flow. When the sheath electrolyte flow-rate approaches the natural aspiration rate induced by the argon gas flow-rate, an approximate ''balance point'' will be reached and the induced laminar flow will approach zero at the electrophoresis capillary tip. In such cases, the pressure differential between the liquid in the sheath flow and the liquid in the capillary approaches zero. Higher sheath flow-rates generate a reverse laminar flow-rate through the electrophoresis capillary [33].

For a fixed nebuliser gas flow-rate, the sheath flow-rate required to eliminate the laminar flow through the electrophoresis capillary was estimated in the following manner. A sample plug (47 nl) from a chromium sample solution ($5 \cdot 10^{-4}$ *M*) is introduced to the electrophoresis capillary and the time required for the plug to migrate the length of capillary can be measured with no voltage applied. Knowing the volume of the capillary (~1.2 μl) and the migration time at a given sheath flow-rate, the laminar flow-rate through the capillary can be calculated. In this manner, a plot of sheath flow-rate vs. laminar flow-rate was recorded and the sheath flow-rate necessary to eliminate the laminar flow can be estimated by extrapolating to zero. Normally the selection of sheath flow-rate is a compromise between analyte resolution and analysis time [33]. For simple systems it is often possible to work with a significant laminar flow-rate towards the detector to minimise the analysis time.

Optimisation of the ICP-MS operating parameters was performed using a $5 \cdot 10^{-4}$ *M* Cr sample solution. One end of the electrophoresis capillary is placed in the Cr sample solution that is drawn through the capillary by induced laminar flow. From experience, it has been found that the optimum nebuliser gas flow setting is ~0.80 l/min [56]. With this setting, the sheath flow-rate (e.g., 50 μl/min) is set to provide a fixed laminar flow-rate (e.g., ~0.1 μl/min) and, therefore, a constant uptake of Cr analyte. The *x*–*y* position of the plasma torch, ion-optic cylinder lens, power and nebuliser gas flow-rate are then fine-tuned.

The physical properties of the separation electrolyte are important, as they will ultimately affect the quality of the separation. In particular, the concentration of the electrolyte chosen should be high enough to provide an electrolyte conductivity that is large compared to the sample solution containing injection volume (plug), but not so large as to cause Joule heating upon application of the external field. The large conductivity difference between sample plug and separation electrolyte ensures a high-voltage gradient across the sample plug and an additional focussing of analyte bands due to electrostacking [57].

The type of electrolyte chosen can be equally as important as its concentration. In order to maintain accurate solution speciation, it is essential that the separation electrolyte does not react or complex significantly with the analyte. In addition, the electrolyte chosen should have a greater (or as large as possible) affinity for any active surface sites along the inner-wall of the capillary than the analyte. This is necessary to minimise analyte–wall interactions and consequently sample loss due to trapping [58]. As a general rule of thumb, the separation electrolyte should have (if possible) a charge greater than the analyte. Typically the more highly charged the electrolyte (i.e., 1+, 2+ or 3+) the smaller the relative sample loss [32,59].

In parallel with the above discussion, Lanthanum based electrolyte solutions have been used in the ion-exchange separation of Cr(III) species to elute the higher order polymeric species [31]. Based upon this demonstrated affinity for exchange sites, a $LaCl_3$ separation electrolyte solution was chosen. The electrolyte concentrations used were 4 or 5 m*M* $LaCl_3$ and were pH modified to between 3 and 6 with HCl (where specified) resulting in electrolyte conductivities between 1100 and 1800 μS. At 30 kV, currents between 10 and 15 μA were observed. The electrolyte conductivity was typically 5× greater than the analyte sample solutions studied. $La(NO_3)_3$ or $La(ClO_4)_3$ electrolyte solutions would probably have made better choices due to the non-complexing nature of the anions. A comparison of La and Na based electrolyte solutions of equivalent conductivity indicated poorer separation efficiency for the Na based separation electrolyte. Working with higher conductivity separation electrolytes should be possible with smaller capillaries, however, this is at the expense of sample size and sensitivity [50,60].

The normal analytical procedure is summarised as follows: With the ICP-MS optimised and running:

(1) the nebuliser gas flow is turned off, (2) the sheath flow-rate turned off, (3) sample is injected and the end of the capillary placed back in the separation electrolyte reservoir, (4) the sheath flow-rate is turned on, (5) the nebuliser gas flow is turned on, (6) the high-voltage power supply is turned on, (7) data acquisition is initiated and (8) upon completion of the run the high-voltage power supply is turned off. The sheath flow-rate is then reduced to facilitate the induced flow of electrolyte through the capillary for flushing purposes until the next run is ready.

4. Results and discussion

4.1. CE–ICP-MS identification of polymeric species and method development

A species distribution diagram for Cr(III) ($5\cdot10^{-4}$ *M*) in the presence of $LaCl_3$ ($4\cdot10^{-3}$ *M*) is shown in Fig. 2 from pH 2 to 7. The plot illustrates that hydrolysis starts to become significant at pH 3 with the formation of $Cr(OH)(H_2O)_5^{2+}$. The rate of formation of the dimer is dependent on the form of the monomer, where formation from, for example, $Cr^{3+} + Cr(OH)^{2+}$ is slow (~300 000×) compared with $Cr(OH)_2^+ + Cr(OH)_2^+$. From the data presented by Stunzi et al. [17], it is estimated that the formation of polymeric species does not become significant until ~pH 4 for a total Cr(III) concentration of $5\cdot10^{-4}$ *M*. Usually, the formation of the dimer precedes the formation of the trimer, which likewise precedes the formation of the tetramer and other higher order polymeric species [16].

Not visible in Fig. 2, is the $CrCl^{2+}$ species distribution profile, which has a maximum that is much less than 1%, indicating that chloride complexation is only a very minor component of the Cr(III) speciation for the conditions described. With hydrolysis, however, chloride complexation may play a greater role [62].

In a common preparatory route for polymeric species [14], a base (NaOH) is added to the stock solution to facilitate hydrolysis and promote polymerisation. The solution is aged for a specified period of time and is then separated into its polymer fractions using ion-exchange chromatography prior

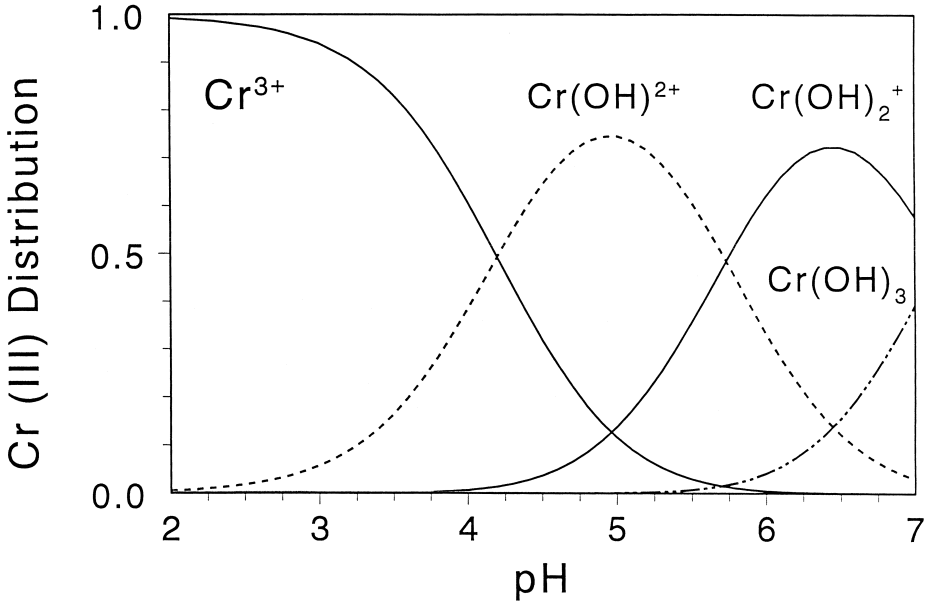

Fig. 2. A Cr(III) ($5\cdot10^{-4}$ *M*) monomer species distribution diagram in the presence 12 m*M* chloride over the pH range 3–7. The data plot was generated using MINTEQA2 [61]. A curve for $CrCl^{2+}$ is also present, however, its relative concentration was less than 1% over the pH ranges studied.

to characterisation or further chemistry. The amount of base added (expressed as equivalents) and the ageing period, will determine the relative speciation at the time of analysis. Stunzi et al. [17] have presented time vs. speciation data on solutions to which 0.8 equiv. of NaOH were added and then allowed to age for over 4 years. They report slow yet significant changes in speciation over these periods indicating a slow attainment of equilibrium.

Using the same principles described above, a series of Cr(III) solutions containing 0, 1 and 2 equiv. of NaOH were prepared, allowed to age 30 days and then analysed using CE–ICP-MS. The data presented in Fig. 3a was generated from a $5 \cdot 10^{-4}$ *M* $CrCl_3$ solution aged in the absence of NaOH, whereas the data presented in Fig. 3b and c were generated from solutions aged in the presence of 0.5 and 1.0 m*M* NaOH, respectively. The results shown in Fig. 3 clearly indicate that there is a change in the speciation of Cr(III) as a function of pH and that the number of species formed increases with pH over the range studied.

There are three peaks present in the electropherogram shown in Fig. 3a, a major peak at 400 s, a minor peak at 365 s and a very weak peak at 345 s. The pH of this solution at the time of measurement was 3.60, which suggests that polymeric species will be present in only a relatively small concentration [17] and that the dominant species (Fig. 2) will be the ''monomer'' equilibrium mixture. Due to the relatively rapid exchange kinetics of this mixture, the monomer fraction will elute with a migration time between that of the pure Cr^{3+} species (low pH, high mobility) and that of the slowest monomer species present, e.g., $Cr(OH)^{2+}$ or $Cr(OH)_2^+$ (high pH, low mobility). The exact time will be related to the relative concentration of these species, dictated by the sample and separation electrolyte pH. Olesik et al. [32,33] have reported relative mobilities of Cr(III) fractions that were dependent on the sample pH and therefore the equilibrium distribution. The more mobile, yet less intense peaks are consistent with the presence of the equilibrium dimer (365 s) and trimer (245 s) species, both of which will have pH dependent equilibrium distributions [14].

Assuming that the dominant peak in Fig. 3a is due to the monomer, then the change in speciation with pH (Fig. 3b and c) would be consistent with a decrease in monomer concentration (peak at ~400 s for Fig. 3a–c) and an increase in the formation of polymeric species. The electropherogram shown in Fig. 3c indicates the presence of as many as eight peaks (species) at a sample solution pH of 4.30. Because the species formed in the higher pH solutions have shorter migration times than the monomer fraction, it is assumed that the polymeric species are formed with increasing charge to size and therefore increasing electrophoretic mobility. Further discussion on the correlation of migration times with polymeric species will be given below.

For comparison, the relative peak areas for the electropherograms shown in Fig. 3 and one not shown, were determined and expressed as percentage fractions of the total Cr peak area calculated in each electropherogram. The results are listed in Table 1. The peaks in Fig. 3a and b have been labelled numerically from 1 to 8. Peaks 1–3 are tentatively assigned to the monomer, dimer and trimer fractions, respectively. In Fig. 3b and c, although it is possible to label all of the peaks, the peaks corresponding to 4 and above have been grouped. Presumably within this fraction, is the tetramer, pentamer and hexamer along with other higher order species. The data clearly shows the shift to increased polymeric content with increased pH. At 2 equiv. of NaOH (Fig. 3c), the electropherogram indicates that the monomer contributes only ~24% of the total Cr present in the sample. These results, although similar in nature with that presented by Stunzi et al. [17], show a larger relative shift from the monomer to polymeric species. This large relative shift favouring the formation of polymeric species may be a natural consequence of the ageing process under the experimental conditions currently employed. We have used a less concentrated sample ($5 \cdot 10^{-4}$ *M*) and more base (2 equiv.), than that reported by Stunzi et al. [17], the later would certainly favour the formation of polymeric species. Alternatively, it could also be attributable to the initial mixing of base with the sample in which localised regions of high pH can exist. As such this may have contributed to the formation of extremely large or colloidal particles that are not amenable (detected) by CE initially (i.e., see Fig. 4b). With time (i.e., 30 days), however, these species may be converted back to smaller (detectable) polymeric species as the pH equilibrates to its lower value.

In addition to pH and concentration, ageing plays

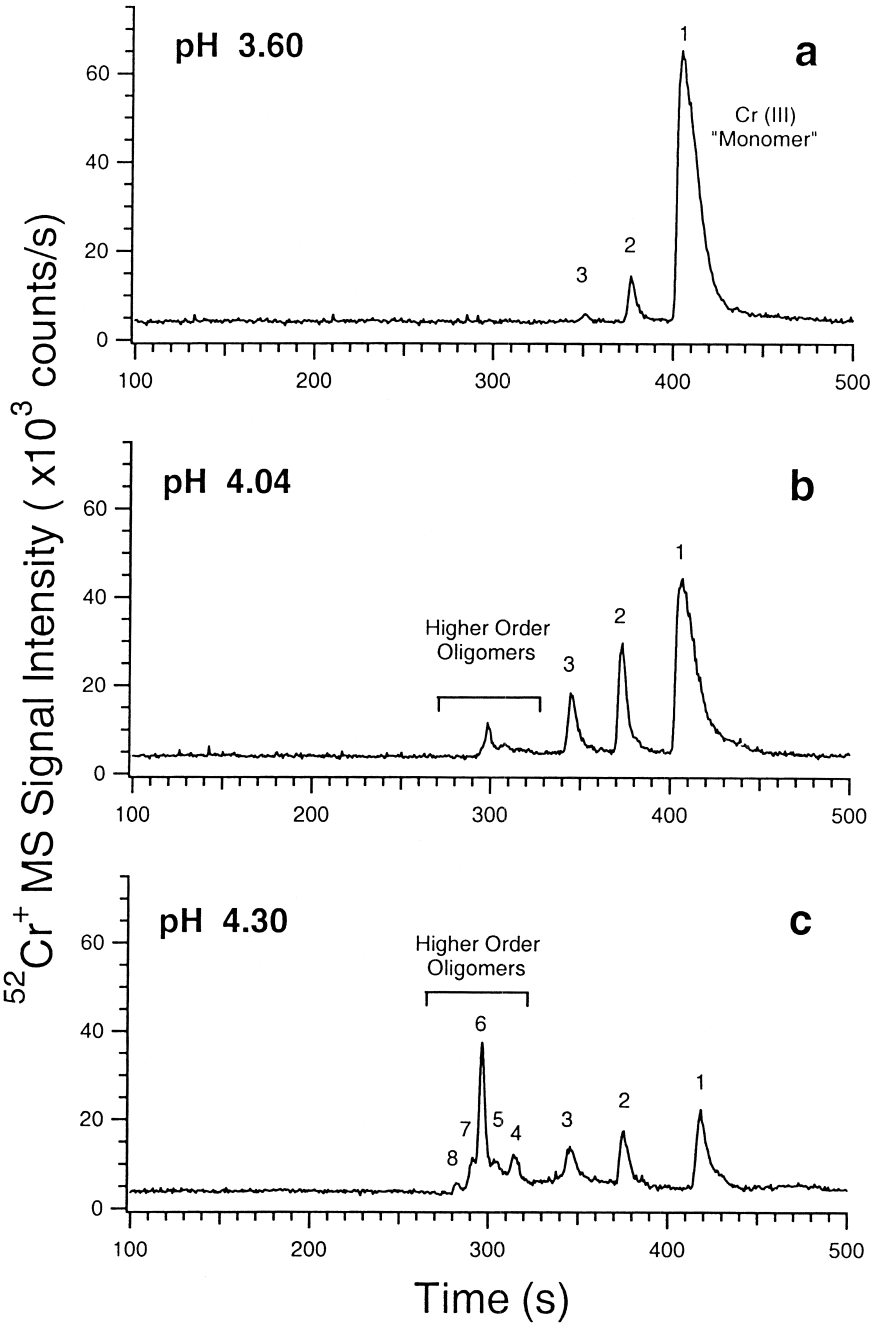

Fig. 3. The effect of pH on the polymeric speciation of Cr(III) as detected by CE–ICP-MS. In all cases the separation and sheath electrolyte was 5 m*M* $LaCl_3$ (pH 5). The sheath flow-rate was set just above the balance point from which the estimated induced laminar flow-rate was ~0.005 μl/min. A $5 \cdot 10^{-4}$ *M* $CrCl_3$ solution was allowed to age 30 days in the presence of (a) 0, (b) 1.0 and (c) 2.0 equiv. of NaOH, corresponding to 0, 0.5 and 1.0 m*M* NaOH, respectively. For further details see Table 1.

Table 1
A comparison of the relative peak areas[a] of the Cr(III) fractions detected in Fig. 3

	pH	Peak 1, monomer	Peak 2, dimer	Peak 3, trimer	Peaks 4+, higher order oligomers
Fig. 3a	3.6	93.19	6.06	0.75	–
Not shown	3.7	91.15	7.67	1.19	–
Fig. 3b	4.0	63.91	16.74	11.51	7.84
Fig. 3c	4.2	23.87	14.66	15.34	46.14

[a] Expressed as a percentage of the total of all $^{52}Cr^{+}$ CE–ICP-MS peak areas in each electropherogram.

an integral part in defining the speciation of Cr(III) in a given system. For freshly prepared solutions the conversion of the monomer to the dimer and the subsequent formation of higher order polymeric species is dependent on pH. At low pH, the formation of the dimer is slow [16] and therefore the sequential formation of the trimer on to higher order polymeric species will also be slower. For solutions that age at a higher pH (base added), the conversion of the monomer into the dimer, trimer, etc. occurs at a faster rate. In either case the formation of polymeric species or ''ageing'' in aqueous solutions is typically characterised by a decrease in solution pH [17]. Qualitatively, it should be possible to follow the species progression within an ageing solution to help facilitate peak assignment in the CE–ICP-MS electropherograms. As such, the ageing of two solutions, one without NaOH added and one with NaOH added, was monitored as a function of time (Fig. 4).

In the first system, a freshly prepared stock solution of $CrCl_3$, was diluted immediately to $5 \cdot 10^{-4}$ *M* in deionised water. From this solution sample aliquots were analysed using CE–ICP-MS over regular periods of time. Initial measurements followed the ageing period over 3 h, the solution was then run periodically after this on separate days, as a result some experimental variation is expected. The results from a selected number of electropherograms are shown in Fig. 4a. The series of electropherograms reveals that initially (~8 min) three species are present and elute at ~330, 350 and 390 s. The third species at 390 s, however, is significantly reduced by 20 min. This speciation is expected based upon the slow exchange (kinetically inert) of Cl in the inner solvation sphere of the chromium monomer resulting in a time dependent (transient) Cr–Cl complex. The more intense peak at ~350 s, again, is most likely due to the monomer equilibrium mixture. After 3 days, only two species are present; the monomer at ~360 s and a more mobile species at 330 s that most likely is the dimer. Considering Fig. 3a to be the eventual product of the ageing mixture, the third more mobile peak at ~340 s is probably a trimer species. The solution pH was recorded for each experimental run, starting at 3.8 it decreased to 3.4 (3 days), which is characteristic of polymerisation processes [14].

In the second system, a freshly prepared stock solution of $CrCl_3$, was diluted immediately to $5 \cdot 10^{-4}$ *M* in presence of a base giving a final concentration of 1 m*M* NaOH. Aliquots of this mixture were measured as a function of time immediately after dilution and selected electropherograms are shown in Fig. 4b. On the first day (20–160 min) the electropherograms reveal the monomer (major) and two other species, possibly the dimer and trimer present initially (20 min). With time, however, the relative intensity of the monomer species decreases and the intensity of the peak at ~360 s starts increasing (90 min). This is consistent with the increased formation of the trimer from the dimer and monomer as the solution ages. At 160 min a more mobile series of peaks starts to become significant between 300 and 350 s. Again, this is consistent with the formation of higher order polymeric species which becomes possible with the formation of the lower mass dimer and trimer (precursors) building blocks. The electropherogram from Fig. 3c collected at 30 days is also included for comparison, highlighting the age dependent progression of solution species to higher order polymeric species. Similar to the data discussed previously (Fig. 4a), the pH of the solution used to generate Fig. 4b decreased over the course of the measurement period. The data are also consistent with that presented by Stunzi et al. [17] in that the

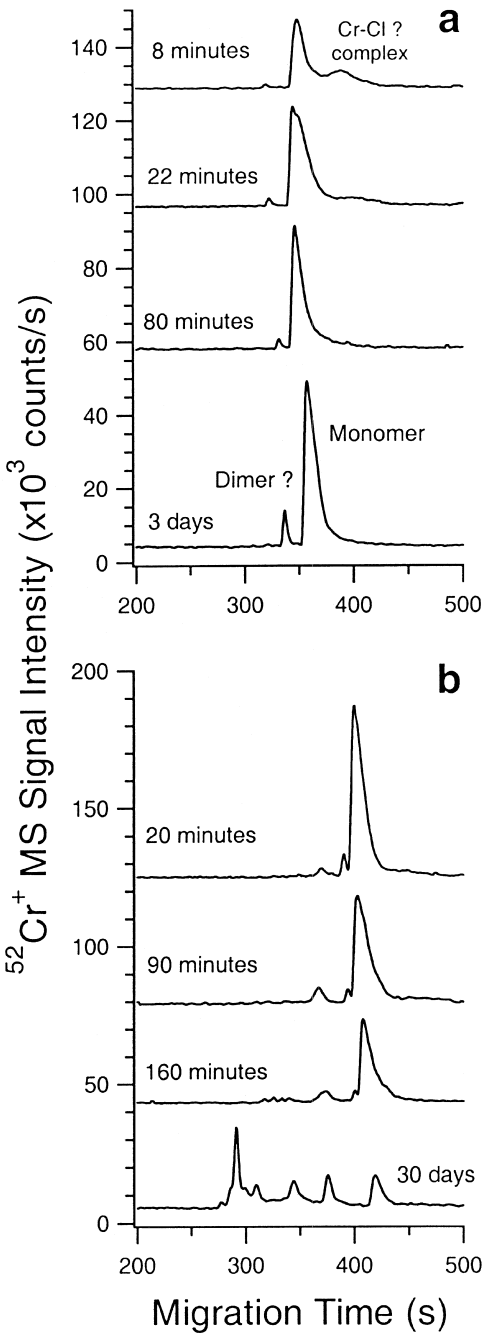

Fig. 4. The effect of sample ageing on the polymeric speciation of Cr(III) as detected by CE–ICP-MS. Sample: $5\cdot10^{-4}$ *M* $CrCl_3$ aged in the presence of (a) 0 and (b) 1 m*M* NaOH. In all cases the separation sheath electrolyte was 5 m*M* $LaCl_3$ (pH 5). The sheath flow-rate was set just above the balance point from which the estimated induced laminar flow-rate was ~0.005 μl/min.

change in monomer concentration as a function of time is more pronounced in solutions with larger amounts of base added. At a lower pH the evolution of oligomers is expected to be small compared with higher pH solutions, which can be in excess of 50% [17].

Even though the $LaCl_3$ separation electrolyte–sheath flow electrolyte has demonstrated its utility for the separation of the hydrolytic Cr(III) species, it also appears to limit the analytical performance of the ICP-MS. In particular, the potential degradation in signal sensitivity due to space-charge effects can be significant. La^{+} (m/z 139) is larger in mass and is delivered to the plasma per unit mass at rates much greater than the analyte (Cr^{+}, m/z 52). For example, consider a 5×10^{-4} *M* sample plug (47 nL) that travels through the capillary under the influence of laminar flow alone (i.e. no external voltage applied). For simplicity, if the peak is assumed to elute with a perfect rectangle or 'plug' like profile with a peak width of 30 s at the base, then during this time ~1 pmol/s analyte is delivered to the nebuliser tip. Over the same time period, the $LaCl_3$ separation electrolyte/sheath flow (4 m*M*) is delivered to the nebuliser tip at a rate of 50 μl/min or ~3000 pmol/s. Assuming a transport rate efficiency of 30% [56] this corresponds to ~1000 pmol/s $LaCl_3$ and ~0.3 pmol/s Cr^{3+} delivered to the plasma on average. For comparison, the typical transport efficiency through a double pass spray chamber with a sample uptake rate of 1 mL/min (typical sample introduction) is only ~1–2%. For a 4m*M* $LaCl_3$ solution, this would correspond to transport rates between 700 and 1400 pmol/s respectively. Therefore, a large amount of lanthanum is introduced into the plasma that may result in significant space charge induced loss of analyte sensitivity. The use of higher shealth flow rates normally associated with increased resolution (decreased induced laminar flow rate) will exacerbate this effect.

An additional consequence of the use of high concentration electrolyte solutions is the gradual accumulation of electrolyte salt deposits on the sampling orifice, skimmer cone and the cylinder ion optic lens. Significant accumulation could degrade the sampling efficiency and hence, analytical performance of the ICP-MS. For $LaCl_3$, significant cloudy white enamel-like deposits become noticeable

on the tip of the skimmer after several hours of operation.

Although the separation electrolyte is required in the electrophoresis capillary, is not essential in the sheath flow. As discussed above, one of the purposes of the sheath flow electrolyte is to provide sufficient conductivity such that a good electrical contact can be made with the grounded stainless steel tubing. Large differences in conductivity between the solution exiting the electrophoresis capillary and the sheath flow electrolyte can lead to additional field gradients that might affect the quality of the separation. With this in mind a dilute nitric acid solution was prepared for use as a sheath electrolyte. The nitric acid sheath flow electrolyte was conductivity matched with the sheath flow electrolyte (e.g., 1200 μS). Results using the dilute HNO_3 sheath flow electrolyte were compared to the standard $LaCl_3$ sheath electrolyte based upon a 47-nl injection of $5 \cdot 10^{-4}$ *M* $CrCl_3$ (pH 2.85). Experimental runs with and without applied voltage were conducted, in both cases the analytical area of the Cr^+ MS signal increased approximately one order of magnitude without any significant change in the migration time or peak shape. The experimental results for the injections where voltage was applied as in a normal analytical run is given in Fig. 5a. Comparison of peak areas with a multi-element solution (e.g., see Table 1) using the same experimental conditions is given in Fig. 5b. For a sheath flow-rate of 50 μl/min this improvement is presumably due to the fact that now only 0.03 μl/min (~1/1700) $LaCl_3$ is delivered to the nebuliser due to induced laminar flow. Although the improvements in sensitivity are consistent with that expected based upon space-charge phenomenon, it should be noted that the ICP-MS ion-optic was optimised only for Cr^+. Using the dilute HNO_3 sheath flow it was also found that the sampler and skimmer cones remained relatively clean and that there was little or no discernible salt accumulation over periods of 8–10 h of operation.

Under the conditions used, a slight positive laminar flow was present in addition to the positive electroosmotic flow. As such, there was a net flow of liquid from the capillary tip into the sheath flow. Although there was little or no significant change in the migration time or peak shapes recorded using simple chemical systems, it is unknown whether there are any deleterious effects due to the pH modification or mixing of the different electrolyte solutions at the electrophoresis capillary tip. It would seem reasonable, however, that matching the counter ion in the separation electrolyte with that of the sheath flow electrolyte would be desirable to minimise any mixing due to the counter-migration of anions with the applied electric field.

A further consideration when using a dilute HNO_3 sheath flow electrolyte for CE–ICP-MS, is that all metal in contact with the charged electrolyte solution should be inert. In particular, to avoid electrochemical contamination of the sheath electrolyte, a platinum tube should replace the stainless steel ground tubing (Fig. 1). In addition, non-conducting materials (plastic based) should be used in place of any metal (brass) connections at the syringe pump. When this precaution is not taken, contamination from the stainless steel or brass fittings can give rise to significant Cr, Fe and Cu contamination. Matrix dependent molecular ion overlaps such as $^{40}Ar^{12}C^+$ (m/z 52) or $^{37}Cl^{16}O^+$ (m/z 53) that have been reported in other Cr ICP-MS literature [63] were not observed here.

4.2. Relative electrophoretic mobility

Using the above method, the relative mobility of Cr(III) species was investigated in more detail. To a freshly prepared multi-element solution (Table 1), containing $CrCl_3$ ($5 \cdot 10^{-4}$ *M*), HCl was added to provide a final concentration of 1 m*M* and a pH of 2.85. The mixture was separated using a 4 m*M* $LaCl_3$ electrolyte that was pH modified to 3. The slight imbalance in pH between the sample and separation electrolyte implies that some pH modification of the labile Cr(III) monomer distribution is possible during the course of the run in addition to the slight modification of any polymeric species acid–base equilibrium distribution. Regardless of this fact, the Cr(III) monomer should exist primarily as the Cr^{3+} aquo-ion, with only minor contributions due to the $Cr(OH)^{2+}$ species. The formation of any polymeric species such as dimer should therefore only occur in small concentrations. In addition, the dimer should exist primarily in its protonated form, $[Cr_2(OH)_2(H_2O)_8^{4+}]$.

The CE–ICP-MS electropherogram of this mixture

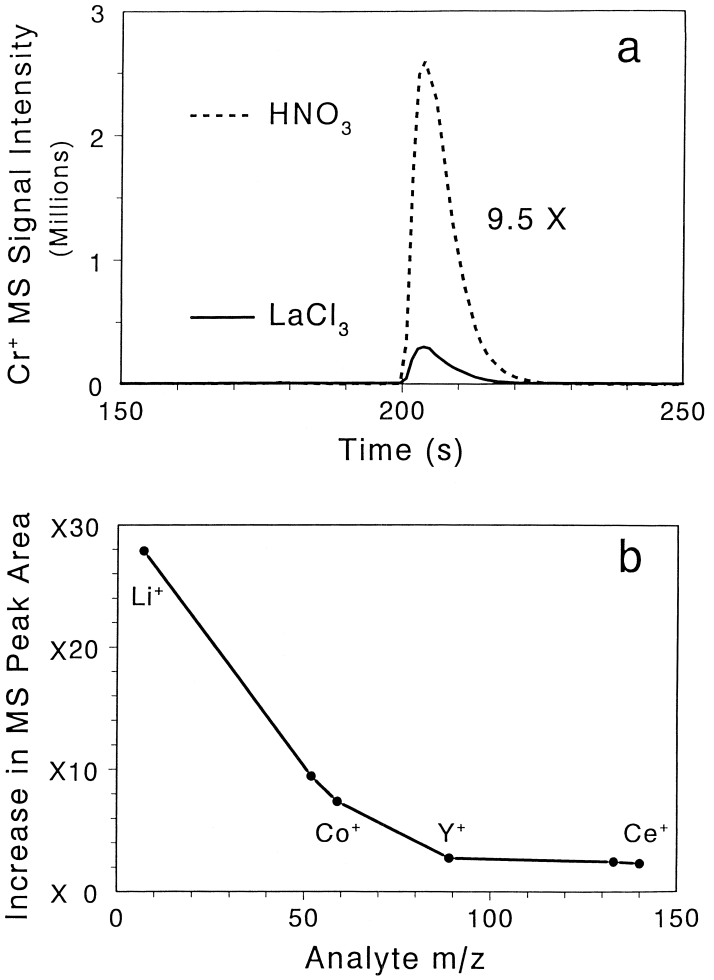

Fig. 5. Effect of sheath flow electrolyte on CE–ICP-MS signal. (a) $^{52}Cr^+$ signal traces recorded from $5 \cdot 10^{-4}$ *M* $CrCl_3$ sample solutions with dilute HNO_3 and $LaCl_3$ (4 m*M*, pH 3) sheath flow electrolyte solutions. The conductivity of both electrolyte solutions is ~1800 μS. Solution pH: 2.85, injection volume: 47 nl, laminar flow-rate: 0.034 μl/min., CE voltage: 30kV, CE current: 10 μA. (b) Change in the peak area recorded for a series of analytes with increasing mass (Table 1) when a dilute HNO_3 sheath flow electrolyte is used compared with an $LaCl_3$ sheath electrolyte. Experimental conditions are the same as Fig. 5a.

is shown in Fig. 6a. The figure clearly indicates that the dominant species present is the monomer with only a very minor contribution by the dimer at 165 s. Also shown in Fig. 6a are a number of ''marker'' species used to gauge the relative mobility of the Cr(III) species. The equivalent ionic conductance of each ion is listed in Table 2. The migration time for the Cr(III) monomer peak is longer than expected based on the equilvalent conductance for the pure Cr^{3+} aquo ion (Fig. 2). As a bench mark for this pH, the monomer fraction elutes before a typical 2+ solution ion (Co^{2+}).

Similar to the monomer, the equilibrium dimer distribution is composed primarily of the highly mobile, fully protonated form, $Cr_2(OH)_2(H_2O)_8^{4+}$, in addition to a smaller concentration of the singly deprotonated form, $Cr_2(OH)_3(H_2O)_7^{3+}$ [14]. Overall, the dimer distribution at this pH has a mobility similar to that of the highly mobile Ce^{3+} aquo-ion.

In Fig. 6b, a similar multi-element solution mix-

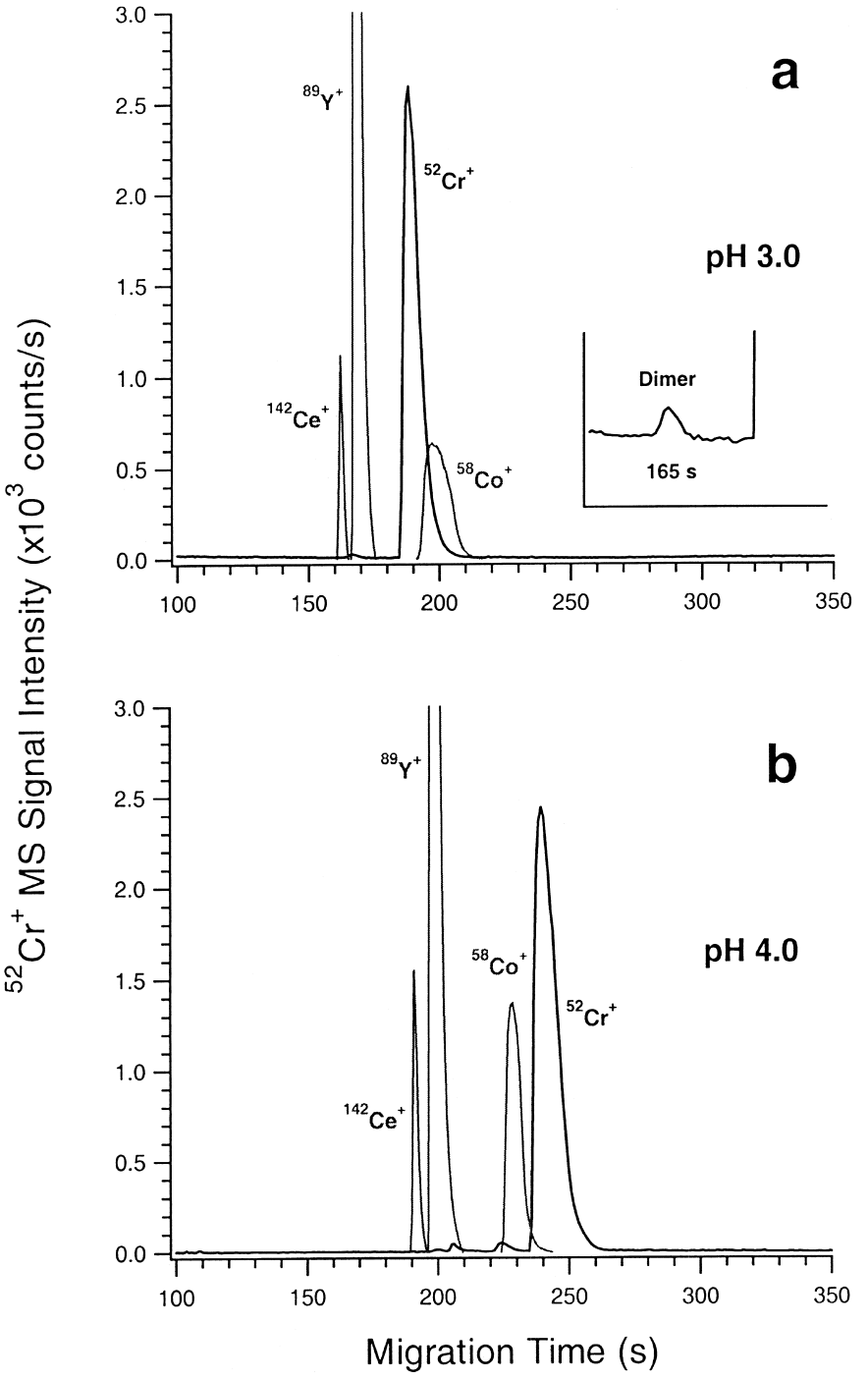

Fig. 6. CE–ICP-MS electropherograms of (a) $CrCl_3$ ($5 \cdot 10^{-4}$ *M*) aged for 2 weeks in the presence of HCl giving a pH of 2.85 at the time of measurement and (b) $CrCl_3$ ($5 \cdot 10^{-4}$ *M*) aged naturally for 2 weeks giving a final pH of 4.0. Each solution contains various electrophoretic mobility markers for reference (Table 2). The separation electrolyte in each case was pH matched ($LaCl_3$, 4 m*M*). The sheath electrolyte was dilute HNO_3 (conductivity matched) generating an induced laminar flow-rate of 0.03 μl/min.

Table 2
A list of the test analytes used and relevant physical parameters

Element	m/z monitored	Concentration ($\times 10^{-4}$ M)	Equivalent ionic conductance $\lambda_i(1 \cdot 10^{-4}$ m^2 S mol$^{-1})$[a]
Li	7	10.0	38.7 (Li^+)
Na	23	5.0	50.1 (Na^+)
Co	59	1.1	55.0 ($1/2Co^{2+}$)
Cr	52	5.0	67.0 ($1/3Cr^{3+}$)
Y	89	1.1	62.0 ($1/3Y^{3+}$)
Ce	142	0.5	69.4 ($1/3Ce^{3+}$)
Cs	133	0.6	77.2 (Cs^+)

[a] From Ref. [69].

ture was aged ''naturally'' for 2 weeks. The separation electrolyte was pH matched to that of the sample solution prior to analysis. In this electropherogram, it is unclear why there is a noticeable difference in the overall migration times for all species. The relative separation between the Ce^{3+}, Y^{3+} and Co^{2+} marker ions, however, changes little as a function of pH, whereas the mobility of the Cr(III) species changes significantly relative to these markers. At pH 4, the monomer equilibrium distribution will shift from primarily the Cr^{3+} aquo-ion to almost an equal concentration of Cr^{3+} and $CrOH^{2+}$, thus reducing the overall mobility of this fraction resulting in migration times longer than the Co^{2+} ion. Because the overall migration time is based upon the relative contribution of the equilibrium species it can probably be assumed that the $Cr(OH)^{2+}$ species has a mobility less than that of Co^{2+} ($\lambda_i = 55$, Table 1). The dimer which elutes at ~225 s, will have longer migration times due to a similar shift in the equilibrium distribution to increasing concentrations of the fully deprotonated forms [i.e., $Cr_2(OH)_3(H_2O)_7^{3+}$ and $Cr_2(OH)_4(H_2O)_6^{2+}$]. The more mobile species eluting at ~200–210 s are most likely that of the trimer (equilibrium distribution) and possibly tetramer. The smaller difference in elution times between the dimer and monomer fractions may be attributable to the larger shifts in the equilibrium distributions for the dimer because of its smaller (more acidic) pK_a values [14].

The data in Fig. 6 illustrates two important points. The first is that the relative migration time of monomer and polymeric species is dependent on the equilibrium distribution, which in turn is dictated by the solution pH. The second, is that regardless of the pH the migration times (mobilities) of the polymeric species are faster than that of the monomer equilibrium distributions.

4.3. IS-MS identification of hydrolytic polymerisation products of Cr(III)

The above CE–ICP-MS method has demonstrated its ability to separate and detect polymeric species as well as provide qualitative assignments to a number of species; direct evidence for the existence of polymeric species, however, is still lacking. One method that has demonstrated great potential for the direct determination of inorganic complexes is ES-MS [64,65]. This is primarily due to its ability to transfer solution phase ions intact into the gas phase for sensitive MS detection. Initial investigations by Van den Bergen et al. [66] of analogous Cr(III) polynuclear species suggest that the determination of Cr(III) oligomers should also be possible. Later investigations by Stewart and Horlick [67] provided only indirect evidence for the presence of polymeric species. The lack of success can be attributed in part to the use of an instrument with limited mass range (<300 u) and sensitivity. In addition, non-aqueous solvents such as methanol were used to dilute analyte test solutions. Although the exact effect of using non-aqueous solvents for the ES-MS measurement of Cr(III) oligomers is unclear, the presence of methanol is thought to suppress the formation of oligomers [6].

In this paper we report some of our preliminary results characterising polymeric Cr(III) species as a function of sample pH and ageing. In our experi-

ments we have used a laboratory-constructed ion-spray source coupled with an PE/Sciex API 300 instrument capable of MS–MS experiments with a ~3000 u mass range. The source has proved ideally suited for the determination of species in purely aqueous solutions that cover a wide range of conductivities [55]. Mass spectra acquired from two different solutions are shown in Fig. 7.

In Fig. 7a, a $5 \cdot 10^{-4}$ *M* $CrCl_3$ solution was prepared by diluting a stock solution in doubly distilled water, the solution was allowed to age for approximately 3 days prior to analysis. The mass spectrum (Q1 scan) was acquired under mild conditions so as not to promote the fragmentation of larger polymeric species. Fig. 7a reveals almost exclusively monomeric species, in particular the solvated singly and double charged reduced species $Cr(OH)(H_2O)_n^{2+}$ and $Cr(OH)_2(H_2O)_n^{+}$, that are typical for these operating conditions and solution pH (3.85) [66]. In addition there is also a series of hydrated Cr–Cl complexes that observed almost exclusively from *m*/*z* 200 and up. These species may be residual of the slow exchange process of the kinetically inert Cr(III) centre, or more likely they were formed as a result of the electrospray process itself. Although the mass spectrum reveals that monomer species are predominant, similar to Fig. 4a, there is also a small contribution by the dimer $Cr_2(OH)_4(H_2O)_6^{2+}$ at *m*/*z* 140, in addition to other more solvated species. At pH 3.85 a significant portion of the dimer will exist in a protonated form ($pK_{a_1} = 3.68$, $pK_{a_2} = 6.04$) [14]. Further charge reduction (hydrolysis) of the dimer in the gas phase also occurs to yield the final charged reduced dimer species recorded by the mass spectrometer. This is to be expected considering that the dimer species was recorded with relatively few H_2O ligands [$Cr_2(OH)_4(H_2O)_6^{2+} \approx 3$ per Cr center], whereas conversion from the singly charge reduced monomer to the doubly charge reduced monomer species occurs with as many as seven H_2O ligands, i.e., at $Cr(OH)(H_2O)_7^{2+}$ (Fig. 7a). The presence of the deprotonated dimer was confirmed using MS–MS. Perhaps a more significant note from this work is that under the conditions employed, the monomer species can be observed with as many as 12 H_2O ligands whereas the dimer species is only partially solvated. Although purely speculative, this may imply that solvent ligands are less strongly bound by the oligomer due to charge delocalisation. If so, then it would partially explain the higher mobility typically observed with the polymeric Cr species in CE. This needs to be explored in more detail before a more definite relationship can be drawn.

In Fig. 7b, a $5 \cdot 10^{-4}$ *M* $CrCl_3$ solution was prepared by diluting a stock solution in deionised water and 1 m*M* NaOH the solution was allowed to age for approximately 3 days prior to analysis. The mass spectrum (Q1 scan) shown was acquired under mild conditions to provide a compromise between conditions that would not promote the fragmentation of larger polymeric species yet would provide a simplified, solvent stripped mass spectrum of the species present. A qualitative comparison with Fig. 6a indicates a significant change in the solution speciation. This is consistent with what would be expected based on the data presented in Figs. 3 and 4. In Fig. 7b the most intense peak is due to the monomer species at *m*/*z* 158. Other, singly charge reduced monomeric species with accompanying solvation are also observed between *m*/*z* 90 and 130. At the higher pH (5.38), of this solution, the equilibrium distribution of the monomer is expected to be ~65% $Cr(OH)^{2+}$, 30% $Cr(OH)_2^{+}$ and 5% Cr^{3+} (Fig. 2), thus favouring the formation of the dimer and other higher order polymeric species. Although not shown, the change in monomer distribution as a function of pH, recorded under similar MS conditions is reflected in the mass spectrum and is consistent with previous work [67].

Fig. 7b reveals the presence of several polymeric species present in the solution, most notably; dimers, trimers, tetramers, pentamers and hexamers. Each species was confirmed by MS–MS studies. Fig. 8 shows a ''blow-up'' of the region from *m*/*z* 225 to 275 (Fig. 7b) acquired with increased resolution and longer integration times (see caption). The figure shows the overlapping tetramer and hexamer distributions, with insets provided for comparison with the theoretical isotopic distribution of select species. Although Fig. 6b indicates that the monomer is the dominant species, to more accurately compare the relative Cr(III) distribution with that of CE–ICP-MS, e.g Figs. 3 or 4, the intensity of each of the polymeric species recorded in Fig. 6b must be multiplied by their respective Cr nuclearity. In this

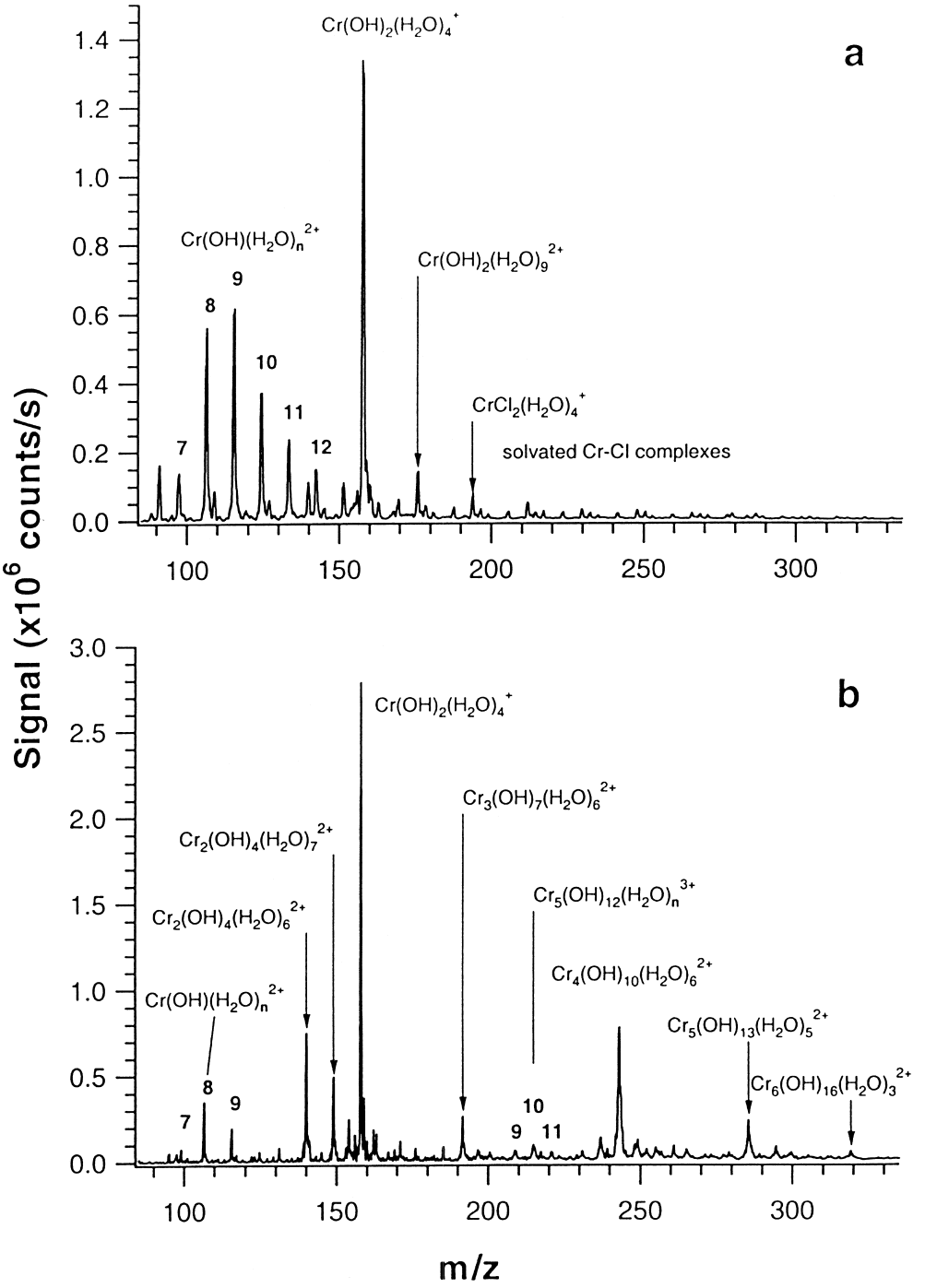

Fig. 7. Electrospray mass spectrum of a purely aqueous solution of $CrCl_3$ ($5 \cdot 10^{-4}$ *M*) with (a) no NaOH added (pH 3.85) and (b) $1 \cdot 10^{-3}$ *M* NaOH added (pH 5.38). The solutions were aged for approximately 3 days.

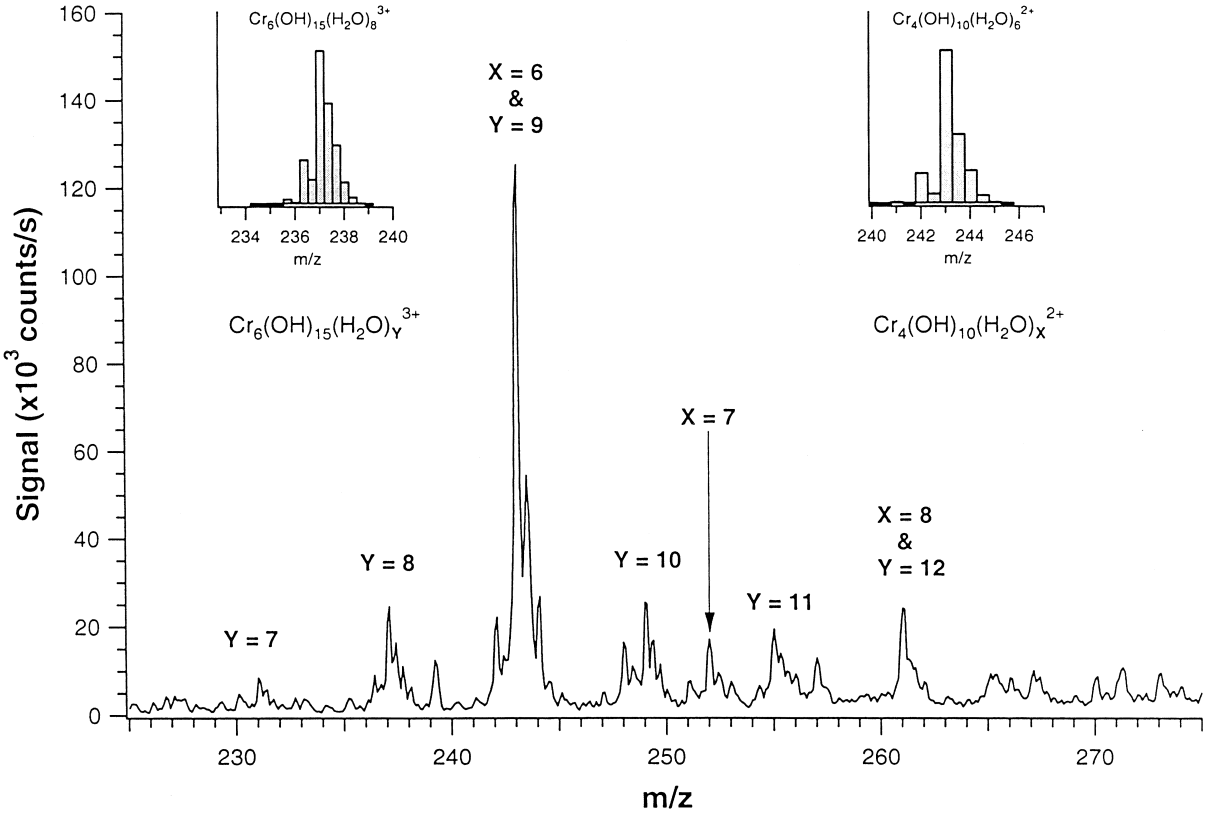

Fig. 8. A close up of the region from m/z 225 to 275 (Fig. 7b) including insets of the isotopic abundance for $Cr_6(OH)_{15}(H_2O)_8^{3+}$ and $Cr_4(OH)_{10}(H_2O)_6^{2+}$. For this experiment, the resolution was adjusted to allow the multiply charged isotope distributions (3+) to be distinguished from each other. The dwell time was increased to 1 s per point.

manner, the tetramer (m/z 243) becomes a significant species having a relative Cr intensity of ~$2.4 \cdot 10^6$ counts/s. Under these solution conditions it is expected that the polymeric species will exist primarily in their deprotonated (hydrolysed) forms in solution, and although their large size should help support a greater charge, gas phase charge reduction does occur under the conditions employed.

The data presented in Figs. 7 and 8 are important as they link the species observed in CE–ICP-MS electropherograms (Figs. 3 and 4) to polymeric species which are present in solution under these conditions. This strongly supports the hypothesis that CE–ICP-MS can be used to separate and detect individual hydrolytic polymerisation products of Cr(III) in aqueous solution. In addition the data presented in Figs. 7 and 8 offer the first direct evidence for the existence of hydrolytic polymerisation products by mass spectrometry. Based on this success a much more thorough ES-MS investigation of these species is currently underway.

5. Conclusions

From the work presented above, a number of important conclusions can be drawn on the use of CE–ICP-MS as a tool for polymeric Cr(III) speciation. (1) CE–ICP-MS can be used to separate and detect monomeric and polymeric Cr(III) species; (2) the species distribution is similar, qualitatively to that predicted in aged and ageing solutions of Cr(III); (3) the various species migrate through the capillary at a rate proportional to their equilibrium distribution in that a single peak may have a migration time that is the concentration weighted

average of more than one species (such as Cr^{3+} and $Cr(OH)^{2+}$) if the kinetics of inter-conversion are rapid enough. In addition, the data indicate that the polymeric species have a greater electrophoretic mobility than the monomer and suggests that they follow the order, trimer>dimer>monomer. More definite assignment of higher order tetrameric, pentameric or hexameric forms is still needed.

The use of auxiliary methods such as IS-MS has independently confirmed the presence of various, expected, monomeric and polymeric species present in solution. Further, the relative Cr(III) speciation as a function of time, pH and concentration are consistent (qualitatively) with that determined in the analogous CE–ICP-MS experiments. Although preliminary in nature, the IS-MS data presented here are significant because they represent a direct way of characterising Cr(III) oligomers in solution. As such, a more in depth study of Cr(III) polymeric species using IS-MS is currently underway.

A final, significant outcome from this work is the development of methodology capable of separating and detecting hydrolytic polymeric species. In particular, the use of element selective detection, allows the use of simple electrolyte systems which do not contribute to a significant change in speciation, sample loss or MS signal suppression. Recognition of this fact, promotes the further development of even more efficient systems. The success of most ion-exchange methods for the separation of different polymer fractions relies on the fact that the polymers are relatively stable at low pH [14]. As such, by running samples under acidic conditions (pH<3), the equilibrium speciation for most species should be shifted to favour almost exclusively the fully protonated forms of the oligomers [reactions (5)–(9)]. In addition to simplifying the polymeric speciation, the use of acidic conditions should further reduce the loss of sample at the walls. Already, Mie et al. [53] have demonstrated that 0.05 *M* HNO_3 can be used to separate Cr(III) and Cr(VI) fractions. Collins et al. [31], however, have used non-complexing mixtures of acidic $La(ClO_4)_3$ to elute higher order polymeric species using ion-exchange chromatography. Both methods, in combination with a dilute HNO_3 sheath-flow electrolyte, present relatively simple and potentially effective ways of separating polymeric species. It is envisaged that other simple systems could be used to separate and detect polymeric ions from other easily hydrolysed elements such as Al or Fe. For example, the ability to use a simple non-complexing medium for the separation and identification of Al^a, Al^b and Al^c fractions is an extremely attractive feature [68].

Although, the above technique has demonstrated great promise, further clarification of the identification or elution order of the various polymeric species is still necessary. Using the method of Stunzi and Marty [14], it should be possible to generate and separate fractions of the various polymeric species. The identity of the fractions can first be confirmed using IS-MS. Once identified, the fractions can be used to correlate the elution times with each polymeric species by spiking the sample solution. The coupling of CE with IS-MS also provides an attractive alternative, as it offers the potential for direct species information with the corresponding elution order.

Acknowledgements

The Perkin-Elmer Corporation is thanked for partial support for the Perkin-Elmer/Sciex ELAN 6000 inductively coupled plasma mass spectrometer. Support for this research was provided in part by Perkin Elmer and PE-Sciex I.I.S. gratefully acknowledges the help and advice provided by Eric Grunwald and Jeffery Kinzer.

References

[1] C.F. Baes, R.E. Mesmer, The Hydrolysis of Cations, Wiley, New York, 1976.
[2] F.Y. Saleh, G.E. Mbamalu, Q.H. Jaradat, C.E. Brungardt, Anal. Chem. 68 (1996) 740.
[3] J. Barnhart, Reg. Toxicol. Pharm. 26 (1997) S3.
[4] A.V. Palwisz, R.A. Kent, U.A. Schneider, C. Jefferson, Environ. Toxicol. Water Qual. 12 (1997) 123.
[5] J.O. Nrigau, in: J.O. Nriagu, E. Nieboer (Eds.), Chromium in the Natural and Human Environments, Wiley, New York, 1988, pp. 81–104, Chapter 3.
[6] S.K. Ibrahim, A. Watson, D.T. Gawne, Trans. IMF 75 (1997) 181.
[7] T. Gotsis, L. Spiccia, K.C. Montgomery, J. Soc. Leather Technol. Chem. 76 (1992) 195.
[8] M.R. Grace, L. Spiccia, Inorg. Chim. Acta 213 (1993) 103.

[9] P. Shu, in: Oil Field Chemistry: Enhanced Recovery and Production Stimulation, ACS, Symposium Series, Vol. 396, American Chemical Society, Washington, DC, 1989, p. 137.
[10] C.L. Dona, D.W. Green, G.P. Willhite, J. Appl. Polym. Sci. 64 (1997) 1381.
[11] E. Nieboer, A.A. Jusys, in: J.O. Nriagu, E. Nieboer (Eds.), Chromium in the Natural and Human Environments, Wiley, New York, 1988, p. 35, Chapter 2.
[12] M. Thompson, R.E. Connick, Inorg. Chem. 20 (1981) 2279.
[13] J.E. Finholt, M. Thompson, R.E. Connick, Inorg. Chem. 20 (1981) 4151.
[14] H. Stunzi, W. Marty, Inorg. Chem. 22 (1983) 2145.
[15] H. Stunzi, F.P. Rotzinger, W. Marty, Inorg. Chem. 23 (1984) 2160.
[16] F.P. Rotzinger, H. Stunzi, W. Marty, Inorg. Chem. 25 (1986) 489.
[17] H. Stunzi, L. Spiccia, F.P. Rotzinger, W. Marty, Inorg. Chem. 28 (1989) 66.
[18] T. Merakis, L. Spiccia, Aus. J. Chem. 42 (1989) 1579.
[19] L. Spiccia, W. Marty, Polyhedron 10 (1991) 619.
[20] L. Spiccia, Polyhedron 10 (1991) 1865.
[21] M.R. Grace, L. Spiccia, Polyhedron 10 (1991) 2389.
[22] S.J. Crimp, L. Spiccia, H.R. Krouse, T.W. Swaddle, Inorg. Chem. 33 (1994) 465.
[23] A. Drljaca, L. Spiccia, Polyhedron 12 (1995) 1653.
[24] A. Drljaca, L. Spiccia, Polyhedron 15 (1996) 2875.
[25] A. Drljaca, L. Spiccia, Polyhedron 15 (1996) 4373.
[26] L. Spiccia, M. Marty, Inorg. Chem. 25 (1986) 266.
[27] L. Spiccia, H. Stoeckli-Evans, W. Marty, R. Giovanoli, Inorg. Chem. 26 (1987) 474.
[28] D. Rai, B.M. Sass, D.A. Moore, Inorg. Chem. 26 (1987) 345.
[29] J.W. Ball, D.K. Nordstrom, J. Chem. Eng. Data 43 (1998) 895.
[30] S.M. Bradley, C.R. Lehr, R.A. Kydd, J. Chem. Soc., Dalton Trans. 9 (1993) 2415.
[31] S.H. Collins, S.H. Pezzin, J.F.L. Rivera, P.S. Bonato, C.C. Windmoller, C. Archundia, K.E. Collins, J. Chromatogr. A 789 (1997) 469.
[32] J.W. Olesik, J.A. Kinzer, S.V. Olesik, Anal. Chem. 67 (1995) 1.
[33] J.A. Kinzer, J.W. Olesik, S.V. Olesik, Anal. Chem. 68 (1996) 3250.
[34] Q. Lu, R.M. Barnes, Michrochem. J. 54 (1996) 129.
[35] P.W. Kirlew, J.A. Caruso, Appl. Spectrosc. 52 (1998) 770.
[36] P.W. Kirlew, M.T.M. Castillano, J.A. Caruso, Spectrochim. Acta B 53 (1998) 221.
[37] K.L. Sutton, C. B'Hymer, J.A. Caruso, J. Anal. Atom. Spectrom. 13 (1998) 885.
[38] B. Michalke, P. Schramel, J. Chromatogr. A 750 (1996) 51.
[39] B. Michalke, P. Schramel, Fresenius J. Anal. Chem. 357 (1997) 594.
[40] B. Michalke, P. Schramel, Analusis 26 (1998) M51.
[41] B. Michalke, P. Schramel, J. Chromatogr. A 807 (1998) 71.
[42] B. Michalke, P. Schramel, Electrophoresis 19 (1998) 270.
[43] B. Michalke, S. Lustig, P. Schramel, Electrophoresis 18 (1997) 196.
[44] S. Lustig, B. Michalke, W. Beck, P. Schramel, Fresenius J. Anal. Chem. 360 (1998) 18.
[45] B. Michalke, P. Schramel, Electrophoresis 19 (1998) 2220.
[46] K.A. Taylor, B.L. Sharp, J.D. Lewis, H.M. Crews, J. Anal. Atom. Spectrom. 13 (1998) 891.
[47] V. Majidi, N.J. Miller-Ihli, Analyst 123 (1998) 803.
[48] V. Majidi, N.J. Miller-Ihli, Analyst 123 (1998) 809.
[49] R.M. Barnes, Fresenius. J. Anal. Chem. 361 (1998) 246.
[50] J.W. Olesik, in J.A. Caruso, K.L. Sutton (Eds.), Elemental Speciation – New Approaches for Trace Element Analysis, Elsevier, 1999, in press.
[51] K.L. Sutton, R.M.C. Sutton, J.A. Caruso, J. Chromatogr. A 789 (1997) 85.
[52] G.K. Zoorob, J.W. McKiernan, J.A. Caruso, Mikrochim. Acta 128 (1998) 145.
[53] E. Mei, H. Ichihashi, W. Gu, S. Yamasaki, Anal. Chem. 69 (1997) 2187.
[54] A.R. Timerbaev, O.P. Semenova, W. Buchberger, G.K. Bonn, Fresenius J. Anal. Chem. 354 (1996) 414.
[55] J.W. Olesik, K.K. Thaxton, S.V. Olesik, J. Anal. Atom. Spectrom. 12 (1997) 507.
[56] J.A. Kinzer, Ph.D. Thesis, Ohio State University, Columbus, OH, 1997.
[57] R.-L. Chien, Anal. Chem. 63 (1991) 2866.
[58] G.O. Roberts, P.H. Rhodes, R.S. Snyder, J. Chromatogr. 480 (1989) 35.
[59] K. Csoban, M. Parkanyi-Berka, P. Joo, Ph. Behra, Colloids Surf. A 141 (1998) 347.
[60] E.J. Grunwald, Capillary Electrophoresis Inductively Coupled Plasma Mass Spectrometry: Detection Limits, Sample Matrix and Metal-Ligand Considerations, M.S. Thesis, The Ohio State University, 1998.
[61] MINTEQA2/PRODAF2, A Geochemical Assessment Model for Environmental Systems, Version 3.11, US Environmental Protection Agency, Athens, GA, 1990.
[62] J.H. Espenson, Inorg. Chem. 8 (1969) 1554.
[63] M. Pantsar-Kallio, P.K.G. Manninen, J. Chromatogr. A 170 (1996) 89.
[64] R. Colton, A. D'Agostino, J.C. Traeger, Mass Spectrom. Rev. 14 (1995) 79.
[65] I.I. Stewart, Spectrochim. Acta B Rev. 55 (1999) (in press).
[66] I.I. Stewart, Spectrochim. Acta B Rev. 54 (1999) 1649–1695.
[67] I.I. Stewart, G. Horlick, J. Anal. Atom. Spectrom. 11 (1996) 1203.
[68] D.R. Gildea, A.M. Phipps, J.H. Ferguson, Inorg. Chem. 16 (1977) 1257.
[69] R.C. West (Ed.), CRC Handbook of Chemistry and Physics, 68th Edition, CRC Press, 1987-1988.